

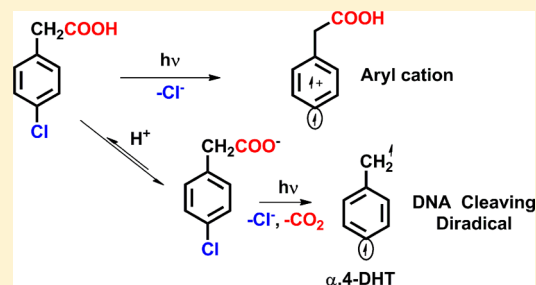
Photogenerated α,n -Didehydrotoluenes from Chlorophenylacetic Acids at Physiological pH

Davide Ravelli, Stefano Protti, and Maurizio Fagnoni*

Photogreen Lab, Department of Chemistry, University of Pavia, Viale Taramelli 12, 27100 Pavia, Italy

S Supporting Information

ABSTRACT: Aromatic diradicals are recognized as promising intermediates for DNA cleavage, but their formation has thus far been limited to the Bergman and Myers–Saito cycloaromatizations. We report here the phototriggered generation of all isomers of the potential DNA-cleaving α,n -didehydrotoluene diradicals at physiological pH, accomplished by the irradiation of chlorophenylacetic acids under mild conditions. The desired diradicals were formed upon photolysis of the chosen aromatic in aqueous phosphate buffer solution (pH = 7.3), with the consecutive elimination of biologically compatible chloride ion and carbon dioxide. Theoretical simulations reveal that the efficient decarboxylation of the primarily generated phenyl cations involves a previously not known diradical structure.



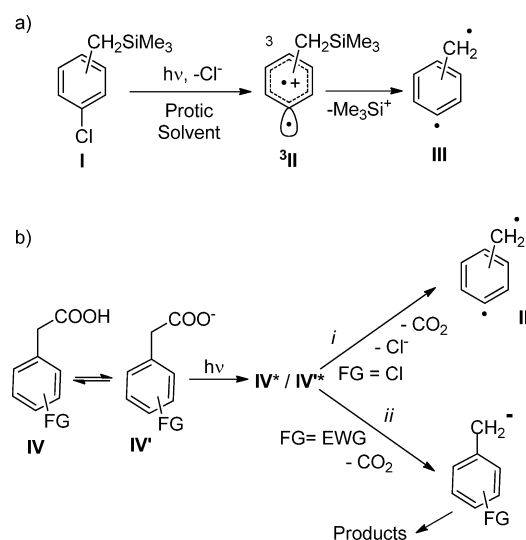
INTRODUCTION

Diradicals are emerging species that find application in several fields, including synthesis, the chemistry of materials, and medicine.¹ With regard to the last field, naturally occurring enyne antibiotics show broad anti-neoplastic activity² due to the formation of a 1,5-didehydroindene or a 1,4-didehydrobenzene diradical via a cycloaromatization process (via a Myers–Saito or a Bergman reaction, respectively).^{3,4} Such diradicals abstract hydrogen atoms from deoxyribose residues in DNA. Accordingly, many efforts have been devoted to the time-consuming synthesis of cyclic enyne-allenes or enediynes that mimic the reactivity of natural compounds, albeit these models have found no practical applications so far.^{5,6}

At any rate, the scope of cycloaromatization is limited since only $\alpha,3$ -didehydrotoluenes ($\alpha,3$ -DHTs) are formed from enyne model compounds via the Myers–Saito reaction.^{5,6} However, we recently demonstrated^{7,8} that all of the three isomeric α,n -DHT ($n = 2–4$) diradicals (**III**, Scheme 1a) are generated by a one-photon-induced double elimination from (chlorobenzyl)trimethylsilanes (**I**). The process involves the consecutive detachment of the chloride anion (forming a triplet phenyl cation, **3II**) and of the trimethylsilyl cation (as an electrofugal group).^{7,8} The chemistry of the generated phenyl cation and the ensuing diradical depended on the medium. In particular, formation of the latter was favored when the polarity of the protic solvent increased, for example, by shifting from neat alcohol to aqueous mixtures. Thus, both the fact that the presence of water improves the generation of DHTs⁷ and the obvious interest in this solvent for a medicinal application prompted us to investigate precursors more soluble in water than chlorobenzylsilanes.

We then reasoned that an alternative electrofugal group could be chosen to impart solubility in an aqueous (in

Scheme 1. (a) Generation of α,n -Didehydrotoluene Diradicals (α,n -DHTs, **III**) via the One-Photon Double Elimination from (n -Chlorobenzyl)trimethylsilanes (**I**) and (b) Photochemical Pathways for Phenylacetic Acids (**IV**)



particular, physiological) environment to the precursor and explored whether aggressive diradicals could be formed by consecutive dechlorination/decarboxylation rather than dechlorination/desilylation. In fact, the carboxylic group serves as an electrofugal group in biosynthetic and other biological processes, as in the isopentenyl pyrophosphate synthesis, in a way functioning as nature's substitute for a silyl group.⁹

Received: October 9, 2014

Published: December 5, 2014

Table 1. Irradiation of Chlorophenylacetic Acids 1a–c^a

1a: R = 4-Cl
1b: R = 3-Cl
1c: R = 2-Cl

2
3a-c, R = Me
5a-c, R = H
4a
6, R = H
7, R = Me
8
9

Substrate	Entry	Solvent	Yield (%)							α,η -DHT derived products (%)		
			2 ^b	3 ^b	4	5	6	7	8		9	
1a $\Phi_{-1} = 0.076^c$ (MeOH) $\Phi_{-1} = 0.26$ (Buffer) ^d	1	CH ₃ OH ^c	30	3a, 6						14	12	40
	2	CH ₃ OH-H ₂ O 9-1 ^c	16	3a, 7						26	16	65
	3	CD ₃ OH-H ₂ O 9-1 ^c	2-d ₁ , 16	3a-d ₃ , 7					7-d ₄ , 2	8-d ₃ , 34	9-d ₂ , 22	72
	4	CH ₃ OH-Buffer ^d 1-9						17	3	12	13	100
	5	CD ₃ OH-Buffer ^d 1-9						41	7-d ₃ , 7		9-d ₂ , 5	100
	6	Buffer ^d				5a, 3	72				1	96
	7	CH ₃ OH, ATMS 0.5 M			4a, 95							
	8	CH ₃ OH, ATMS 0.5 M ^c			4a, 95							
1b $\Phi_{-1} = 0.32$ (Buffer) ^c	9	CH ₃ OH ^c	60	3b, 11								0
	10	CH ₃ OH-H ₂ O 9-1 ^c	50	3b, 13								0
	11	CH ₃ OH-Buffer ^d 1-9	1			5b, 47	34	8				47
	12	Buffer ^d				5b, 53	45					46
1c $\Phi_{-1} = 0.21$ (Buffer) ^c	13	CH ₃ OH ^c	81	3c, 6								0
	14	CH ₃ OH-H ₂ O 9-1 ^c	55	3c, 12								0
	15	CH ₃ OH-Buffer ^d 1-9	7	3c, 5		5c, 14	23	<1		1		49
	16	Buffer ^d				5c, 26	36					58

^aIrradiation conditions: **1a–c** (5×10^{-3} M in the chosen solvent), irradiated at 254 nm (4×15 W Hg lamps), $t_{\text{irr}} = 20$ min (>70% **1a–c** consumption; yields based on consumed **1**). ^bQuantified by HPLC analysis, eluant: MeCN/water (pH = 1.6) 25/75, flux 0.8 mL min⁻¹. ^cCs₂CO₃ (5×10^{-3} M) added. ^dBuffer = 0.05 M aqueous phosphate buffer solution at pH = 7.3.

Recently, the use of a carboxylic moiety as a leaving group in synthesis has gained much attention in metal-mediated cross-coupling reactions,^{10–14} in the defunctionalization of organic compounds induced by enzymes (e.g., decarboxylase),¹⁵ and in photoinduced electron transfer processes.^{16,17}

We thus decided to test *n*-chlorophenylacetic acids (**IV**, FG = Cl, Scheme 1b) in the search for a new class of promising, readily prepared antitumor compounds able to form diradicals under physiological conditions when triggered by light. Interestingly, harmless and stable fragments (chloride ion and CO₂) would be expelled. Obviously, this would be a pH-dependent process, in which the elimination of carbon dioxide from the phenylacetate anion (**IV'**) is expected to be more favorable than from the free acid.

This approach (Scheme 1b, path *i*) would be successful only if alternative photodecarboxylation pathways do not compete with dechlorination. Actually, several largely used NSAIDs (non-steroidal anti-inflammatory drugs; e.g., ibuprofen)^{18–21} containing the ArCH(R)COOH moiety are known to cause adverse photosensitivity responses when susceptible patients are exposed to sunlight.²² In this case, homolytic cleavage of the CH₂–COOH bond was found to be the main pathway for the decarboxylation of phenylacetic acid.²³ The photoreactivity of these acids was found to be enhanced in the anionic form, to an extent that varied with the substituents present on the aromatic ring.^{18,19} Thus, photolysis of carboxylates **IV'** proceeded via the direct photoelimination of carbon dioxide to give a benzyl anion (Scheme 1b, path *ii*), and the consumption of **IV'** was

generally low when FG = H or an electron-donating group,^{9,18–21} where it proceeded via the first singlet excited state (S₁). The decarboxylation efficiency dramatically increased when FG = –NO₂ or –COCH₃, where it proceeded via the first triplet excited state (T₁) and yielded a strongly stabilized benzyl anion.

Our surmise was that the presence of a chlorine atom on the aromatic ring would increase the intersystem crossing (ISC) efficiency,²⁴ preventing any photoreaction from the S₁ state and, in addition, that the CH₂COOH/CH₂COO[–] substituent in chlorophenylacetic acids would be sufficiently electron-donating to allow the photoheterolysis of the Ar–Cl bond. In fact, the CH₂COO[–] group has an electron-donor ability comparable to a Me group,²⁵ and since a triplet phenyl cation was smoothly formed by photolysis of 4-chlorotoluene,²⁶ the generation of the corresponding cation from photoheterolysis of the Ar–Cl bond in the 4-chlorophenylacetate anion should be feasible. There is an early report in the literature that irradiation in water of chlorophenylacetic acid isomers, used as models for the herbicide Fenac, led mainly to dechlorinated products.²⁷

RESULTS

In this work, we report the pH-dependent photochemical behavior in protic aqueous media of the three isomeric *n*-chlorophenylacetic acids **1a–c** (Table 1) and the corresponding carboxylate anions **1'a–c**, supported by theoretical

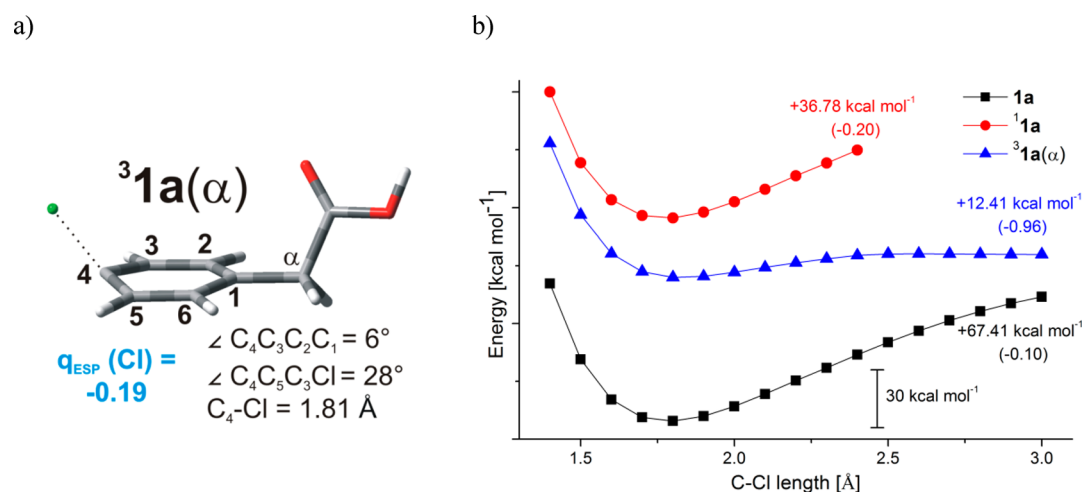


Figure 1. (a) Optimized geometry at the CASSCF/6-31G(d) level and relevant parameters for ${}^3\mathbf{1a}(\alpha)$. ESP charge (q_{ESP}) for the Cl atom at the equilibrium geometry is shown, as derived from single-point calculation in bulk water. (b) Potential energy curves for $\mathbf{1a}$, ${}^1\mathbf{1a}$, and ${}^3\mathbf{1a}(\alpha)$ at the CASSCF/6-31G(d) level of theory in bulk water (see Table S2 for details). The values reported refer to the energy change for the last point of each curve with respect to the equilibrium geometry; in parentheses, the ESP charges for the Cl atom at the same point are reported.

calculations aimed at the rationalization of the observed reactivity.

Experimental Study. First notice that no significant differences in the UV absorption spectra of $\mathbf{1a}$ in methanol and aqueous phosphate buffer were observed (see Supporting Information Figure S1). The irradiation experiments performed are gathered in Table 1, along with the obtained results.

Dechlorination took place when 4-chlorophenylacetic acid $\mathbf{1a}$ ($5 \times 10^{-3} \text{ M}$) was irradiated ($\lambda = 254 \text{ nm}$, 4 lamps) in neat methanol, yielding a mixture of phenylacetic acid ($\mathbf{2}$, 44%) and 4-methoxyphenylacetic acid ($\mathbf{3a}$, 25%).

We then examined the photoreactivity of carboxylate $\mathbf{1}'\mathbf{a}$. In basic methanol ($\text{C}_2\text{CO}_3 = 0.05 \text{ M}$, entry 1), significant amounts of products resulting from both dechlorination and decarboxylation (phenethyl alcohol $\mathbf{8}$ and 1,2-diphenylethane $\mathbf{9}$) were formed at the expense of $\mathbf{2}$ and $\mathbf{3a}$. Compounds $\mathbf{8}$ and $\mathbf{9}$ are diagnostic for the formation of an $\alpha,4$ -DHT intermediate, as previously reported by our group.^{7,8} The process was quite inefficient, however, with a disappearance quantum yield (Φ_{-1}) of 0.076. The presence of water in the reaction medium (MeOH/water 9/1; entry 2) did not change the nature of the products formed but had a marked impact on their distribution, making the products formed through $\alpha,4$ -DHT ($\mathbf{8} + \mathbf{9}$) predominant. No effect resulted from replacing CH_3OH with CD_3OH (entry 3). The presence of a $-\text{COOH}$ group allowed the photoreactivity to be tested in a 1/9 MeOH/aqueous phosphate buffer (pH = 7.3) mixture, in which compound $\mathbf{1a}$ was completely soluble (Table 1, entry 4). In this medium, the results changed dramatically and irradiation led to the exclusive formation of dechlorinated and decarboxylated compounds, that is $\mathbf{8}$, $\mathbf{9}$, and benzyl alcohol $\mathbf{6}$ in comparable yields, along with a minor amount (3%) of methyl benzyl ether $\mathbf{7}$. Irradiation of $\mathbf{1a}$ in a 1/9 CD_3OH /buffer mixture (entry 5) led to the disappearance of $\mathbf{8}$ from the products and to a significant decrease of $\mathbf{9-d}_2$ (down to 5% yield) in favor of $\mathbf{6}$ (from 17 up to 41%) and of deuterated methyl benzyl ether $\mathbf{7-d}_3$. This supported the operation of a primary isotope effect, as suggested by Myers²⁹ and the key role of hydrogen abstraction by the DHT in determining the product distribution. Finally, when the same reaction was carried out in neat buffer to mimic physiological conditions (entry 6), benzyl alcohol $\mathbf{6}$ (72%) was

found to be an almost exclusive product along with small amounts of $\mathbf{9}$ (1%) and of 4-hydroxyphenylacetic acid $\mathbf{5a}$ (3%). In addition, the consumption of $\mathbf{1a}$ under the latter conditions ($\Phi_{-1} = 0.26$) was markedly enhanced with respect to neat methanol.

The photochemistry observed for the isomeric acids $\mathbf{1b}$ and $\mathbf{1c}$ is quite similar to that of $\mathbf{1a}$. Photoreduction to $\mathbf{2}$ and photosolvolysis were the preferred paths for both the *meta*- and the *ortho*-isomers in both basic methanol and 9/1 methanol/water (entries 9, 10 and 13, 14). When switched to the 1/9 methanol/buffer mixture and neat buffer with no methanol (entries 11, 12 and 15, 16), photoreductive dechlorination to $\mathbf{2}$ was dwarfed in favor of photosolvolysis (with the formation of 3- or 2-hydroxyphenyl acetic acids $\mathbf{5b,c}$ in up to 53% yield) and of the generation of the corresponding $\alpha,3$ - and $\alpha,2$ -DHTs, as evidenced by the formation of benzyl alcohol $\mathbf{6}$ in high yield. The use of neat buffer as the reaction medium leveled the photoreactivity of the three chlorophenylacetic acid isomers $\mathbf{1a-c}$, and they exhibited comparable quantum yields for photodecomposition ($\Phi_{-1} = 0.2-0.3$).

As a mechanistic test, the irradiation of $\mathbf{1a}$ was carried out in the presence of allyltrimethylsilane (ATMS, 0.5 M, entries 7 and 8).^{7,30} In this case, irradiation caused the exclusive formation of 4-(2-propenyl)phenylacetic acid $\mathbf{4a}$ (95% yield) at the expense of $\mathbf{2}$ and $\mathbf{3a}$. Likewise, $\mathbf{4a}$ was the exclusive product when the reaction was carried out in the presence of ATMS and C_2CO_3 , in which case the carboxylate anion $\mathbf{1}'\mathbf{a}$ was the prevalent form.

Irradiations of phenylacetic acid ($\mathbf{2}$) and 4-methoxyphenylacetic acid ($\mathbf{4}$) in basic methanol and in buffer have been likewise carried out to exclude competitive pathways in the formation of α,n -DHTs. As a result, the photorelease of carbon dioxide from dechlorinated acids $\mathbf{2}$ and $\mathbf{4}$ is a side process that can take place but did not markedly affect the final product distribution (see Supporting Information for details).

Computational Study. Calculations were then carried out in bulk water (C-PCM solvation model) for modeling the dechlorination of acid $\mathbf{1a}$ (taken as a model) to give a phenyl cation. The level of theory chosen involved a multiconfigurational approach, namely, the complete active space self-consistent field (CASSCF; also capable of handling excited

states), which was further refined by corrections at the MP2 level. A detailed description of computational analysis has been included in the Supporting Information (see Chapter 2). The choice of the active space depended on the structure considered.

As for the C–Cl bond cleavage from the precursor, the modeling focused on the role of the aromatic moiety and of the substituents attached to the ring. Thus, a (10,10) active space was adopted, including the 3π and the $3\pi^*$ orbitals of the aromatic as well as the two σ/σ^* pairs of the C–Cl and the C_α –COOH bonds. We first investigated the geometry of the ground state (**1a**; Figure S2a), the lowest lying singlet ($^1\mathbf{1a}$; Figure S2b), and triplet ($^3\mathbf{1a}$; Figures 1 and S2c,d) excited states. A marked distortion from planarity of the aromatic ring was observed only for $^3\mathbf{1a}$. Two different conformations exhibited nonplanarity, one with the chlorine atom and the carboxylic group on the same side of the aromatic ring (designed as “ α ”; Figures 1a and S2c), and the other with the chlorine and carboxylic acid on opposite sides (“ β ”; Figure S2d). The two conformations are close in energy (ca. 69 kcal mol⁻¹ above the ground state), with the α structure slightly more stable than the β (see Table S1). It may be noted that in $^3\mathbf{1a}(\alpha)$ C₄ sticks out of the aromatic system, with a C₄–C₃–C₂–C₁ dihedral angle of 6°, and the C₄–Cl bond is bent further upward by an angle of 28° with respect to the C₄–C₅–C₃ plane and is significantly elongated, from 1.78 Å (for **1a**) to 1.81 Å. A negative charge likewise develops at the chlorine atom (–0.19).

The potential energy curves reported in Figure 1b (see also Table S2) show the energy variation occurring upon stretching the C₄–Cl bond in the three different states considered above. It is apparent that in triplet $^3\mathbf{1a}$ an increase in the bond length up to 3 Å causes only a modest increase of energy (ca. 12 kcal mol⁻¹) and a marked charge separation. By contrast, imposing the same deformation to the C–Cl bond in either ground (**1a**) or excited ($^1\mathbf{1a}$) singlet states results in a much higher energy increase, with no significant negative charge localization at the chlorine atom. This is consistent with our surmise that heterolytic C–Cl bond cleavage will occur from the lowest triplet state of 4-chlorophenylacetic acid.²⁸

The analysis was then extended to phenylacetates **1'a**–**c**, where two paths were considered, involving loss of chloride anion and CO₂. As for the former, when adopting the same active space used for **1a**, calculations on **1'a** indicate no difference with the ionic state of the carboxyl function, with similar results in terms of geometry of the different states (Figure S3), as well as for the potential energy curves with respect to the C–Cl bond stretching and for charge localization on the chlorine atom (Tables S3 and S4 and Figure S4a). The same holds for the isomeric carboxylates **1'b** and **1'c** (see Supporting Information Tables S3 and S4 and Figures S4b, S5, and S6).

We wondered, however, whether the lone pair at the carboxylate moiety might affect the dechlorination step from the triplet state of **1'a** (with the β conformer here more stable than the α). Unfortunately, the computational cost prevented inclusion of the lone pair into the above-defined active space (which would result in an overall (12,11) active space). A satisfactory analysis was, however, obtained through a simplified computational approach, where only the lone pair at the carboxylate group and the relevant orbitals of the aromatic system were included in the active space (see section 3.1 in Supporting Information). This computational study revealed that two different states concur with the description of the C₄–

Cl bond cleavage. In particular, with a small stretching of the bond (up to a 2.3 Å length) in $^3\mathbf{1'a}(\beta)$, the structure was best described as a “zwitterion” (hereafter named as $^3\mathbf{10'a}^z$, Table S5 and Figure 2), where a marked charge separation in the

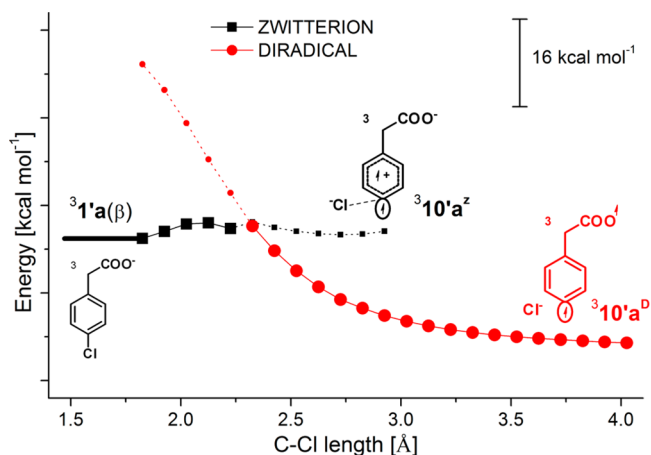


Figure 2. Energy profile upon chloride anion removal from $^3\mathbf{1'a}(\beta)$ at the CASSCF/6-31G(d) level of theory in bulk water (see Table S5 and section 3.1 in Supporting Information for details).

organic fragment is observed. Further stretching of the C–Cl bond, however, led to a surface crossing to a diradical structure (hereafter named as $^3\mathbf{10'a}^d$). As for the energetic profile, this process confronts a very small barrier (a few kcal mol⁻¹) and then proceeds downhill after the surface crossing.

As for the decarboxylation of **1'a**, the computational analysis predicted a large barrier for the cleavage of the C_α–COO⁻ bond (ca. 29 kcal mol⁻¹) from the triplet state to give the corresponding benzyl anion (see section 3.2 in Supporting Information).

With the aim of understanding the actual pathway involved in the processes observed, we modeled computationally the intermediates arising after loss of the chloride anion from **1a** (hereafter named **10a**) adopting a (8,9) active space, including the aromatic system (3π and $3\pi^*$ orbitals), the σ/σ^* couple of the C_α–COOH bond, and the orbital at the dicoordinated carbon (see Supporting Information for further details). Likewise, the structures of **10'a**–**c** were modeled considering (as in precursor **1'a**) the inclusion of the carboxylate group orbitals in the active space. Thus, an overall (12,12) active space was used (see again Supporting Information), comprising the same orbitals adopted for **10a** and the whole carboxylate moiety.

Noteworthy, the molecular structures of $^1,^3\mathbf{10a}$ closely resemble those of alkyl-substituted phenyl cations.²⁶ The calculations predict that in both spin species the phenyl ring is planar, with $^1\mathbf{10a}$ showing a sort of cumulene character at the dicoordinated carbon (with a $\pi^6\sigma^0$ electronic structure), while in $^3\mathbf{10a}$, the ring is more close to a regular hexagon ($\pi^5\sigma^1$ electronic structure, see Figure 3a, where the shape of the two SOMOs is reported).

The ground state of **10a** is the singlet, with a rather large S–T gap (ca. 12 kcal mol⁻¹; see Figure 4a and Tables S7 and S8 for details). The computational investigation established, however, that the situation is completely different for intermediates **10'a**–**c** that are diradical structures with the two SOMOs located predominantly at the dicoordinated carbon and at the carboxylic group, regardless of the isomer

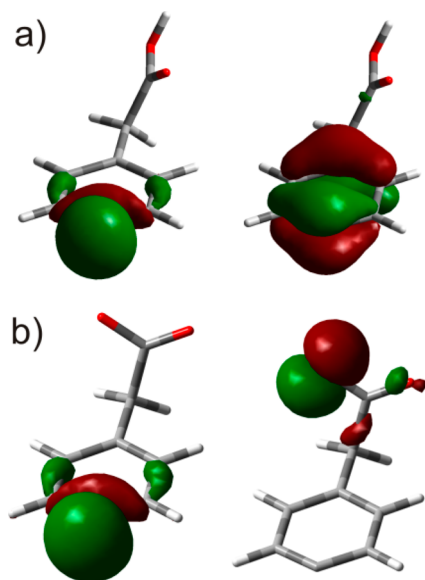


Figure 3. Singly occupied molecular orbitals (SOMOs) for (a) 310a and (b) ${}^{1,3}10'a$, as determined from CPCM-CASSCF/6-31G(d) calculations in bulk water.

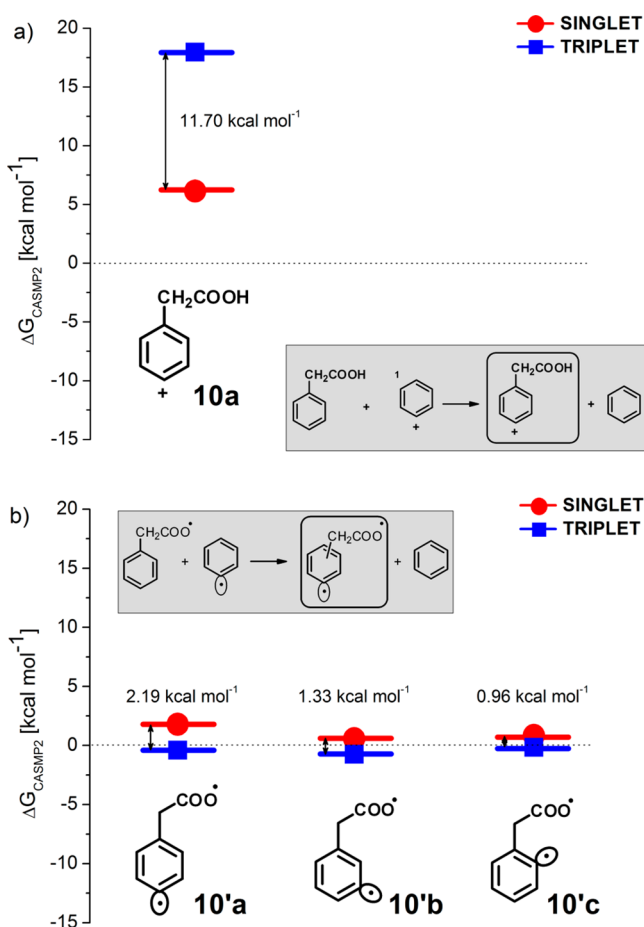


Figure 4. Relative energy of (a) ${}^{1,3}10a$ and (b) ${}^{1,3}10'a-c$ according to the isodesmic equations reported as the inset.

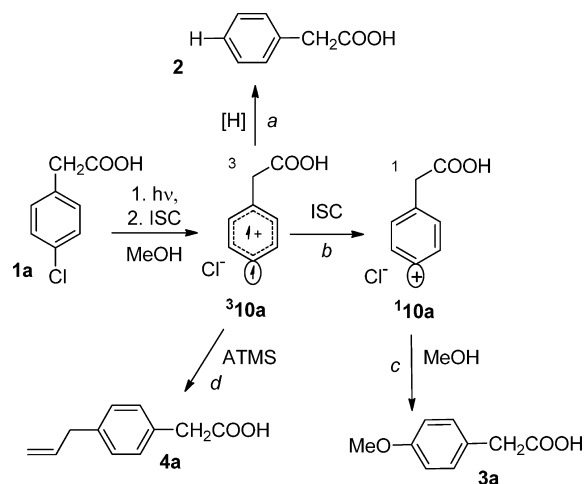
or of the spin state (whether singlet or triplet, Figure 3b). The relative energies of these intermediates have been carefully evaluated. Contrary to cations ${}^{1,3}10a$, ${}^{1,3}10'a-c$ and ${}^310'a-c$ are almost isoenergetic, resulting in ground state triplets with very

small S–T gaps (see Figure 4b and Tables S9 and S10 for details). As for the decarboxylation of ${}^{1,3}10'a-c$ (see Tables S11 and S12), it was shown to occur via a well-defined transition state (tagged TSC), describing the cleavage of the $C_\alpha-COO'$ bond during an overall exoergonic process (see Tables S13–S15 and Figures S9–S11 for details). The observed energy changes are reported in Table S12 and demonstrate that loss of CO_2 from $10'a-c$ occurs with very low activation energies (4.10–8.42 kcal mol $^{-1}$), with parameters similar to those observed for phenylacetoxy radical $2'$ (4.82 kcal mol $^{-1}$ at the same level of theory; see Table S16 and Figure S12), which is well-known to undergo facile decarboxylation.³¹

DISCUSSION

The above experimental observations are corroborated by computational results, and the competing pathways in the photochemistry of carboxylic acids **1a–c** and of carboxylates **1'a–c** are represented in Schemes 2 and 3 for the *para*-derivatives **1a** and **1'a**, respectively.

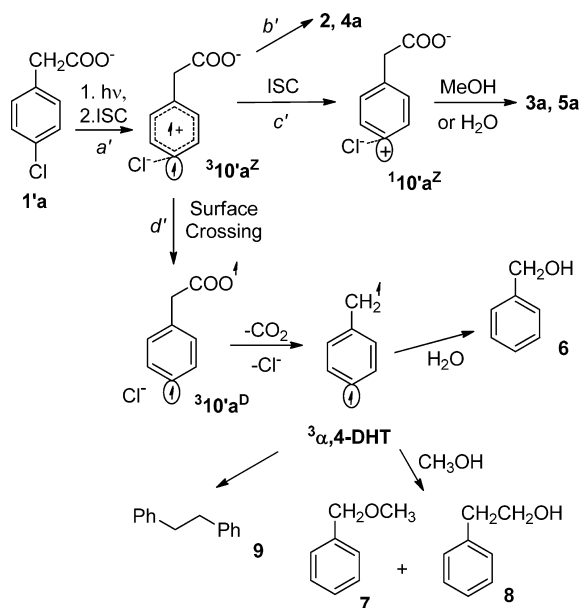
Scheme 2. Photoreactivity of 4-Chlorophenylacetic Acid **1a** (ATMS = Allyltrimethylsilane)



In the framework of the known photochemistry of aryl chlorides, these results suggest that photolysis of **1a** generates triplet phenyl cation 310a as the initial intermediate (by heterolytic fragmentation of triplet 31a). This intermediate abstracts a hydrogen atom from the solvent to give phenylacetic acid **2** (Scheme 2, path *a*). A competitive pathway is ISC, which yields the more stable singlet cation 110a (path *b*), from which 4-methoxyphenylacetic acid **3a** is formed by solvent addition (path *c*). On the other hand, in the presence of ATMS, trapping of 310a takes place faster than both reduction and ISC, and **4a** is obtained exclusively (path *d*). Irradiation of carboxylate **1'a** caused again the heterolysis of the Ar–Cl bond in the triplet state (Scheme 3, path *a'*), but now yielding a triplet zwitterion intermediate that is closely associated with chloride ion (${}^310'a^z$).

The close similarity with the behavior of 310a fully supports the role of intermediate ${}^310'a^z$ (with radical/radical cation character at the aromatic moiety), showing the typical reactivity of triplet phenyl cations, viz. hydrogen abstraction from the solvent and trapping by ATMS (path *b'*), in competition with intersystem crossing (path *c'*), to give ${}^110'a^z$ and compounds **3a** and **5a** from it. However, computational data also support

Scheme 3. Chemical Pathways Involved in the Photoreactivity of the 4-Chlorophenylacetate Anion (1'a)



the role of surface crossing that makes the diradical form $^310'a^D$ the most stable one when chloride is at a larger distance (path d'). The diradical structure is obviously the ideal precursor for CO₂ detachment, and indeed, only a low-energy barrier is required for this process (less than 5 kcal mol⁻¹, with an expected rate around 10¹⁰ s⁻¹, as previously determined for 2').³¹ Thus, access to $^310'a^D$ plays a key role in the ensuing formation of the corresponding $\alpha,4$ -DHT.

Water is known to improve the efficiency of photoinduced Ar–Cl cleavage and also to stabilize the triplet phenyl cation formed.³² Stabilization of triplet phenyl cation may increase the chances of competing paths, such as ISC to the corresponding singlets in some cases (particularly in $10'b,c$), preventing CO₂ loss due to the high reactivity of these singlets with the reaction medium. Accordingly, solvolysis products accounted for ca. 50% of the resulting mass balance arising from **1b** and **1c** in neat buffer. On the other hand, cations $^310'a-c^Z$ are easily reduced in MeOH (a hydrogen-donating solvent), yielding dechlorinated phenylacetic acids as the main products in all cases. The generation of α,n -DHTs is maximized when the leaving group and the benzylic function are *para* to each other (compound **1a**), as was previously observed in the case of chlorobenzylsilanes.^{7,8}

As for the chemistry of the formed α,n -DHTs, the dual behavior (diradical and ionic) of such species is apparent from Table 1.³³ The fastest reaction is hydrogen abstraction from methanol to yield a benzyl radical and the final products from it (alcohol **8** and bibenzyl **9** via a diradical pathway). This reaction is subjected to a clear primary isotope effect (see entries 4 and 5, Table 1). Thus, product distribution arising from the α,n -DHT in CD₃OH buffer (1:9) resulted in the preferential formation of polar products such as alcohol **6** and ether **7** at the expense of the radical product **8**.

CONCLUSION

In conclusion, this work demonstrates that aggressive diradicals (α,n -DHTs) can be easily obtained via a double elimination sequence by absorption of a photon from inexpensive and

readily available substituted phenylacetic acids. Calculations give insight in the sequence of events involved, confirming that the first step is dechlorination. Nucleophiles such as Cl⁻ and water stabilize the phenyl cation, giving room to competing processes, but the absence of hydrogen donors made chlorophenylacetates excellent precursors for DHTs (or at least for the *para*-isomer). This fact, along with the solubility in water, militates in favor of the choice of these derivatives as the active moiety of a new class of photoactivatable therapeutics,³⁴ and it is hoped that this work will lay the foundations for the development of sound pharmaceutically active leads.

EXPERIMENTAL SECTION

The photochemical reactions were performed by using nitrogen-purged solutions in quartz tubes in a multilamp reactor equipped with four Hg lamps (15 W each, emission centered at 254 nm) for the irradiation. Quantitative determination for compounds of interest was carried out by means of HPLC (2–3, 5) and GC (6–9) calibration curves. Quantum yields were measured at 254 nm (1 Hg lamp, 15 W).

Synthesis of 4-(2-Propenyl)phenylacetic acid (4a). A solution of **1a** (85 mg, 0.5 mmol, 0.005 M), Cs₂CO₃ (156 mg, 0.5 mmol, 0.005 M), allyltrimethylsilane (8.05 mL, 50 mmol, 0.5 M) in MeOH was irradiated at 254 nm for 1 h. The solvent was evaporated, and the resulting residue was dissolved in water, acidified at pH = 3 by acetic acid, and extracted with ether (3 × 20 mL). Organic phases were combined, dried over Na₂SO₄, and the solvent evaporated under vacuum. Purification by column chromatography of the residue afforded 76 mg of **4a** (viscous oil, 86% yield): ¹H NMR (δ , CDCl₃) 3.40–3.45 (d, 2H, *J* = 7 Hz), 3.65 (s, 2H), 5.10–5.15 (m, 2H), 5.95–6.00 (m, 1H), 7.20–7.30 (AA'BB', 4H), 10.80 (br s, 1H); ¹³C NMR (δ , CDCl₃) 40.8 (CH₂), 41.6 (CH₂), 116.8 (CH₂), 129.6 (CH), 130.3 (CH), 131.9, 138.5 (CH), 140.1, 179.1; IR (ν /cm⁻¹) 3050, 2955, 1701, 1408, 909, 837. Anal. Calcd for C₁₁H₁₂O₂: C, 74.98; H, 6.86. Found: C, 75.0; H, 6.9. GC-MS (*m/z*): 177 (5), 176 (45), 131 (100), 117(45), 91 (45).

ASSOCIATED CONTENT

Supporting Information

Experimental procedures, sample spectra; optimized geometries, energies and CASSCF output data for all of the structures involved in this work. This material is available free of charge via the Internet at <http://pubs.acs.org>.

AUTHOR INFORMATION

Corresponding Author

*Fax: +39 0382 987323. Tel. +39 0382 987198. E-mail: fagnoni@unipv.it.

Notes

The authors declare no competing financial interest.

ACKNOWLEDGMENTS

This work was supported by the Fondazione Cariplo (Grant 2011-1839). S.P. acknowledges MIUR, Rome (FIRB-Futuro in Ricerca 2008 project RBF08J78Q), for financial support. We thank Prof. A. Albini (University of Pavia) and P. Hoggard (Santa Clara University) for fruitful discussions. We are grateful to B. Mannucci and C. Nicola (Centro Grandi Strumenti-Pavia) for the valuable assistance. This work was funded by the CINECA Supercomputer Center, with computer time granted by ISCRA projects (code: HP10CZEHG6, HP10C6PCC2, and HP10C3CPWN).

REFERENCES

- (1) Abe, M. *Chem. Rev.* **2013**, *113*, 7011–7088.

- (2) Maeda, H. *Anticancer Res.* **1981**, *1*, 175–186.
- (3) Gredičak, M.; Jerič, I. *Acta Pharm.* **2007**, *57*, 133–150.
- (4) Smith, A. L.; Nicolaou, K. C. *J. Med. Chem.* **1996**, *39*, 2103–2117.
- (5) Kar, M.; Basak, A. *Chem. Rev.* **2007**, *107*, 2861–2890.
- (6) Breiner, B.; Kaya, K.; Roy, S.; Yang, W.-Y.; Alabugin, I. V. *Org. Biomol. Chem.* **2012**, *10*, 3974–3987.
- (7) (a) Protti, S.; Ravelli, D.; Mannucci, B.; Albini, A.; Fagnoni, M. *Angew. Chem., Int. Ed.* **2012**, *51*, 8577–8580. (b) Protti, S.; Ravelli, D.; Fagnoni, M.; Albini, A. *Pure Appl. Chem.* **2013**, *85*, 1479–1486. (c) Raviola, C.; Ravelli, D.; Protti, S.; Fagnoni, M. *J. Am. Chem. Soc.* **2014**, *136*, 13874–13881.
- (8) Ravelli, D.; Protti, S.; Fagnoni, M.; Albini, A. *J. Org. Chem.* **2013**, *78*, 3814–3820.
- (9) Meiggs, T. O.; Grossweiner, L. I.; Miller, S. I. *J. Am. Chem. Soc.* **1972**, *94*, 7981–7986.
- (10) Gooßen, L. J.; Rodriguez, N.; Gooßen, K. *Angew. Chem., Int. Ed.* **2008**, *47*, 3100–3120.
- (11) Rodriguez, N.; Gooßen, L. J. *Chem. Soc. Rev.* **2011**, *40*, 5030–5048.
- (12) Bonesi, S.; Fagnoni, M. *Chem.—Eur. J.* **2010**, *16*, 13572–13589.
- (13) Song, Q.; Feng, Q.; Zhou, M. *Org. Lett.* **2013**, *15*, 5990–5993.
- (14) Feng, Q.; Song, Q. *J. Org. Chem.* **2014**, *79*, 1867–1871.
- (15) Kourist, R.; Guterl, J.-K.; Miyamoto, K.; Sieber, V. *ChemCatChem* **2014**, *6*, 689–701.
- (16) See for example: Oelgemöller, M.; Griesbeck, A. G. *J. Photochem. Photobiol. C* **2002**, *3*, 109–127.
- (17) *Photochemically-Generated Intermediates in Synthesis*; Albini, A., Fagnoni, M., Eds.; John Wiley & Sons: Hoboken, NJ, 2013.
- (18) Lukeman, M. Photodecarboxylation of Arylacetic Acids. In *CRC Handbook of Organic Photochemistry and Photobiology*, 3rd ed.; Griesbeck, A., Oelgemöller, M., Ghetti, F., Eds.; CRC Press: Boca Raton, FL, 2012; pp 715–726.
- (19) Boscà, F.; Marin, M. L.; Miranda, M. A. Photodecarboxylation of Acids and Lactones: Antiinflammatory Drugs. In *CRC Handbook of Organic Photochemistry and Photobiology*, 2nd ed.; Horspool, W., Lenci, F., Eds.; CRC Press: Boca Raton, FL, 2004; pp 641–6410.
- (20) Castell, J. V.; Gomez-L, M. J.; Miranda, M. A.; Morera, I. M. *Photochem. Photobiol.* **1987**, *46*, 991–996.
- (21) Moore, D. E.; Chappuis, P. P. *Photochem. Photobiol.* **1988**, *47*, 173–180.
- (22) Moore, D. E. *Drug Safety* **2002**, *25*, 345–372.
- (23) Epling, G. A.; Lopes, A. J. *J. Am. Chem. Soc.* **1977**, *99*, 2700–2704.
- (24) Previtali, C. M.; Ebbesen, T. W. *J. Photochem.* **1985**, *30*, 259–267.
- (25) Hansch, C.; Leo, A.; Taft, R. W. *Chem. Rev.* **1991**, *91*, 165–195.
- (26) Qrareya, H.; Raviola, C.; Protti, S.; Fagnoni, M.; Albini, A. *J. Org. Chem.* **2013**, *78*, 6016–6024.
- (27) Crosby, D. G.; Leitis, E. *J. Agric. Food Chem.* **1969**, *17*, 1036–1040.
- (28) The occurrence of a heterolytic cleavage of the Ar–Cl bond from triplet state aryl halides has found computational and experimental evidences. See for instance: Raviola, C.; Protti, S.; Ravelli, D.; Mella, M.; Albini, A.; Fagnoni, M. *J. Org. Chem.* **2012**, *77*, 9094–9101 and ref 26.
- (29) Myers, A. G.; Dragovic, P. S.; Kuo, E. Y. *J. Am. Chem. Soc.* **1992**, *114*, 9369–9386.
- (30) Dichiarante, V.; Fagnoni, M. *Synlett* **2008**, 787–800.
- (31) Abel, B.; Assmann, J.; Buback, M.; Grimm, C.; Kling, M.; Schmatz, S.; Schroeder, J.; Witte, T. *J. Phys. Chem. A* **2003**, *107*, 9499–9510.
- (32) Manet, I.; Monti, S.; Bortolus, P.; Fagnoni, M.; Albini, A. *Chem.—Eur. J.* **2005**, *11*, 4274–4282.
- (33) (a) For reviews on the diradical/zwitterion dichotomy in synthesis, see: Mohamed, R. K.; Peterson, P. W.; Alabugin, I. V. *Chem. Rev.* **2013**, *113*, 7089–7129. (b) Peterson, P. W.; Mohamed, R. K.; Alabugin, I. V. *Eur. J. Org. Chem.* **2013**, 2505–2527.
- (34) Velema, W. A.; Szymanski, W.; Feringa, B. L. *J. Am. Chem. Soc.* **2014**, *136*, 2178–2191.